Vibrational autoionization in H_2: Vibrational branching ratios and photoelectron angular distributions near the $v^+=3$ threshold

J. L. Dehmer and P. M. Dehmer
Argonne National Laboratory, Argonne, Illinois 60439

J. B. West, M. A. Hayes, and M. R. F. Siggel
Daresbury Laboratory, Daresbury, Warrington, WA4 4AD, United Kingdom

A. C. Parr
National Institute for Standards and Technology, Gaithersburg, Maryland 20899

(Received 5 August 1992; accepted 24 August 1992)

Vibrational branching ratios and photoelectron angular distributions are reported for photoionization of normal (the equilibrium ortho/para mixture) hydrogen in the region just above the $v^+=3$ ionization limit. This region contains a number of vibrationally autoionizing Rydberg states, and the goal of the work was to observe experimentally the characteristic behavior associated with the decay of these states that was predicted by Raoult and Jungen [J. Chem. Phys. **74**, 3388 (1981)] on the basis of an MQDT (multichannel quantum defect theory) calculation on para-H_2 ($J''=0$). We have indeed observed that vibrational autoionization strongly favors the ionization channel representing the minimum change in the vibrational state of the ion core, as predicted. We also observed a sharp reduction in the photoelectron asymmetry of the $v^+=3$ (and, to a lesser extent, the $v^+=2$) ionization channel for resonant photoionization. Hence, qualitative agreement with theory is observed; however, a quantitative comparison now requires an extended calculation that includes the additional rotational levels that were populated under the present experimental conditions.

I. INTRODUCTION

A central aspect of molecular physics is the understanding of those dynamics that arise from the joint motion of electrons and nuclei in molecular fields. The dominant concepts concerning such systems are the Franck–Condon approximation[1,2] and the Born–Oppenheimer approximation,[1,3] which stress the independence of the motions of the light electrons and the relatively massive nuclei in a field that varies adiabatically with the nuclear coordinates. However, for many important molecular phenomena, e.g., vibrational autoionization, electronic predissociation, internal conversion, intersystem crossing, and chemical reactions involving two or more potential surfaces, one must go beyond these approximations and deal directly with the exchange of energy and angular momentum between the light and heavy particles.

A process that is explicitly non-Franck–Condon and non-Born–Oppenheimer in nature is vibrational autoionization. This process typically involves a Rydberg state in which the excited Rydberg electron is bound in the Coulomb field of a vibrationally excited ion core, which has sufficient vibrational energy to ionize the Rydberg electron if the excess vibrational energy is transferred to the loosely bound electron. This transfer can occur during periodic close collisions between the Rydberg electron and the ion core. During such a collision, the electron is accelerated by the strong potential in the core, thus allowing it to exchange energy with the vibrating nuclei more efficiently. The excitation of such a Rydberg state via photoabsorption is a resonant process that is often prominently displayed against a nonresonant background. Hence, the study of vibrational autoionization provides a way to study the dynamics of energy exchange between electronic and nuclear motions.

Vibrational autoionization dominates the vacuum ultraviolet spectrum of molecular hydrogen,[4] which, since it is also theoretically tractable, is the best prototype for studying this uniquely molecular mechanism. In the early 1980s, Raoult and Jungen published an elegant multichannel quantum defect (MQDT) calculation[5] of vibrational autoionization in H_2 that agreed extremely well with the high-resolution total photoionization cross section.[6] They also made many predictions concerning several complementary observables, e.g., rotational and vibrational branching ratios and photoelectron angular distributions. Among these observations were the quantitative illustration of the earlier prediction[7] that vibrational autoionization strongly favors the smallest change in vibrational quantum number as well as the demonstration of localized departures from this propensity rule. Also predicted was a sharp reduction of photoelectron asymmetry in the immediate vicinity of such resonances caused by a transfer of the asymmetry of the dipole excitation process from the photoelectron to the ion core during the resonance lifetime. A third prediction was that resonance effects on the photoelectron asymmetry parameter β extend significantly beyond the resonance halfwidth.

These calculations are considered very accurate and represent a cornerstone of molecular physics, yet many aspects of the calculations have never been tested experimentally. This is very important because, as we are frequently reminded, different observables reflect the dynamics of a process differently, and agreement between experiment and theory in one parameter, particularly an

Downloaded 22 Aug 2006 to 129.6.168.231. Redistribution subject to AIP license or copyright, see http://jcp.aip.org/jcp/copyright.jsp

integrated quantity, does not necessarily indicate a satisfactory understanding of the process. Testing the predictions of Raoult and Jungen[5] requires angle-resolved photoelectron spectroscopy in the vicinity of the first few vibrational ionization limits of H_2. The high-resolution, high-intensity, vacuum ultraviolet light source needed for such single-photon measurements has only recently become available with synchrotron radiation. Only two previous single-photon studies have attempted to determine vibrational branching ratios following autoionization of Rydberg states of H_2. Berkowitz and Chupka[8] measured the distribution of photoelectrons from several unresolved groups of autoionizing peaks by using a retarding-field electron energy analyzer; however, only a few of the most intense features in the spectrum were studied. Later, Dehmer and Chupka[9] indirectly determined the final vibrational state distributions following the decay of approximately 100 autoionizing states by measuring the relative cross sections for $H_2^+ + He(Ne) \rightarrow HeH^+(NeH^+) + H$, reactions that are very sensitive to the vibrational level of H_2^+. The results of both studies were in accord with the vibrational propensity rule, but neither allowed a direct or detailed investigation of the spectral variation of the branching ratios or symmetry parameters as a function of v^+. More recently, double resonance spectroscopy via the $E,F\,^1\Sigma_g^+$ intermediate state has been used to determine branching ratios for vibrational autoionization of the *np* Rydberg states near the $v^+=2$ ionization threshold;[10] however, full MQDT calculations for this process have not yet been published, so a direct comparison between theory and experiment was not possible.

Here we present our initial attempt to test the predictions of Raoult and Jungen.[5] We have performed vibrationally and angularly resolved photoelectron spectroscopy on room-temperature, normal (the equilibrium ortho–para mixture) H_2 just above the $v^+=3$ threshold (763–765 Å) at a wavelength resolution of $\sim$0.18 Å. This wavelength range was chosen because it was the highest energy region characterized by Raoult and Jungen[5] and therefore produced the largest number of vibrational ionization channels. The use of room-temperature, normal H_2 introduces rotational states not present in the calculation and thus requires new calculations before quantitative comparisons between experiment and theory can be made; however, we anticipate our conclusions by noting that qualitative comparisons at the vibrational level are possible for trends in key quantities such as vibrational branching ratios and photoelectron angular distributions.

II. EXPERIMENT

The electron spectrometer system used in this study comprised two hemispherical electron analyzers, each positioned to detect electrons ejected at right angles relative to the horizontal photon beam. One analyzer was fixed in position and accepted electrons ejected horizontally; the other was rotatable about the light beam through an angular range of a little more than 90° from a vertical orientation. The angular acceptance of each analyzer was limited by an aperture in the entrance lens to approximately ± 2 deg. To enhance the sensitivity of the spectrometers, area detectors of the resistive anode type were mounted at the exit plane of the hemispheres. A complete description of the electron spectrometer system has been published previously by Parr *et al.*[11]

The hydrogen sample gas was introduced into the experimental chamber through a 0.25 mm i.d. effusive molecular beam source. A 2 mm i.d. capillary light guide channeled the vacuum ultraviolet radiation from the exit slit of the optical monochromator to a point near the gas outlet to form an ionization region "viewed" by both analyzers. The vacuum ultraviolet radiation was provided by the Synchrotron Radiation Source at Daresbury Laboratory, a 2 GeV electron storage ring. Light was focused onto the entrance slit of a McPherson 5-m near-normal-incidence monochromator, which provided photon fluxes of 10^{10} photons/s in a 0.18 Å bandpass in the wavelength region of interest (763–765 Å). The normal incidence monochromator and its performance have been described by Holland *et al.*,[12] and the beamline to which this instrument was attached has been described by West and Padmore.[13]

The radiation from the exit slit of the monochromator was elliptically polarized with the major axis of the ellipse in the horizontal plane. The degree of polarization was determined by using an analyzer incorporating three gold coated mirrors that was attached to the rotating analyzer. The principle of its use has been described by Horton *et al.*[14] A tungsten mesh served as a flux monitor for the radiation entering this detector, and a tungsten plate was used to measure the intensity after the three reflections. From measurements made at 0° and 90° and from a knowledge of the reflectivities of gold for parallel and perpendicular incident light, it was straightforward to calculate the polarization. The polarization was 0.62 ± 0.02 over the small photon wavelength range of this experiment.

The transmission function (or detection efficiency) of each electron spectrometer was determined as a function of the photoelectron energy and the angle of ejection by using the known photoionization cross sections and angular distributions of the rare gases. The electron signal was corrected for the variation of incident light flux, which was measured by the incident flux monitor, the tungsten mesh in the polarization analyzer. The variation of the efficiency of this detector with photon energy was measured in a separate experiment. The angular distribution of the photoelectrons for dipole excitation of randomly oriented molecules is given by the expression[15]

$$\frac{d\sigma}{d\Omega} = \frac{\sigma}{4\pi}\left[1 + \beta/4(3p\cos 2\theta + 1)\right], \tag{1}$$

where the photoelectron asymmetry parameter β completely characterizes the photoelectron angular distribution. In this expression, p is the polarization of the incoming light, θ is the angle between the major polarization axis and the ejected electron direction, and σ is the partial cross section for that channel. Since helium was used for the angular calibrations in these experiments, β is known to have a value of 2; thus the spectrometer calibration in this

Downloaded 22 Aug 2006 to 129.6.168.231. Redistribution subject to AIP license or copyright, see http://jcp.aip.org/jcp/copyright.jsp

measurement does not depend on measured values of the asymmetry parameter β.

The raw data were corrected for the energy response and relative efficiency of the electron energy analyzers, and the intensities in the vibrational peaks were determined by summing the counts in each peak. Peak fitting was unnecessary, since the electron spectrometer resolution of 40 meV readily resolved the individual vibrational components of the $H_2^+X\,^2\Sigma_g^+$ photoelectron band. Furthermore, the background intensity was low and easily subtracted. This procedure eliminated any dependence of the final results on peak shape, which became somewhat distorted at very low electron energies.

The asymmetry parameter β for each vibrational component of the electronic transition was then determined from Eq. (1). Once β was known, the intensity integrated over all θ for a given vibrational component was determined. This intensity is proportional to the partial cross section and can be used to calculate branching ratios, defined here as the intensity of a particular vibrational component divided by the sum of the intensity of all the vibrational components observed. If the total cross section for the all of the vibrational components of the electronic transition at a particular photon energy is known, it is straightforward to calculate the partial cross sections. Here we have chosen to present the branching ratios for direct comparison to the theoretical results.

The above procedures were used to calibrate the data with the following exception. The intensities in the $v^+=3$ vibrational component could not be determined by using this procedure, because the relative analyzer efficiency is not well characterized for electron kinetic energies below 100 meV. For this vibrational component, we constrained our data to the theoretical β values of Raoult and Jungen[5] at two nonresonant energies, the highest and lowest photon energies examined, to determine an empirical calibration of the $v^+=3$ intensity ratio for the two analyzers. Using this correction, we derived the branching ratios and β values at the intermediate photon energies within the resonance structure. This procedure increases the uncertainty in the absolute β values for this channel; however the relative shape of the β curve in this small region is considered reliable. The branching ratios were insensitive to this calibration procedure.

III. RESULTS AND DISCUSSION

A. Spectroscopic background

The photoabsorption spectrum of H_2 is notoriously complex. At low principal quantum numbers, the spectrum consists of series of $np\sigma\,^1\Sigma_u^+$ and $np\pi\,^1\Pi_u$ Rydberg states; however, as n increases there is a transition from Hund's case (b) in which the orbital angular momentum l is strongly coupled to the internuclear axis to Hund's case (d) in which the orbital angular momentum l is strongly coupled to the axis of nuclear rotation. For large n, the separation into well-resolved $^1\Sigma_u^+$ and $^1\Pi_u$ Rydberg states is no longer observed, but rather the rotational levels of the Rydberg states are ordered solely on the basis of the rotational level of the ion core to which they converge. Perturbations between series are often intense and result in significant energy level shifts and intensity variations from those predicted by the simple Rydberg formula. Indeed, although the vacuum ultraviolet spectrum has been known for more than 60 years,[16] the severity of these perturbations prohibited the complete analysis of the spectrum until only recently, when MQDT was applied to the problem.[4–6,17]

The excitation process in the present experiment can be summarized as

$$\begin{aligned} &H_2X\,^1\Sigma_g^+,v''=0,\ J'' \\ &\quad\rightarrow[(H_2^+X\,^2\Sigma_g^+)np,v',J'] \\ &\quad\rightarrow H_2^+X\,^2\Sigma_g^+,v^+,\bar{N}^+ + e. \end{aligned} \tag{2}$$

Ionization may be via a resonant process (e.g., via the Rydberg state shown in brackets), or it may be direct. Levels of the ground state are labeled by double primes, levels of the autoionizing Rydberg states (if present) are labeled by single primes, and levels of the ion are labeled by a superscript +. The total angular momentum minus the nuclear and electron spins for the ion core in the Rydberg state is denoted N^+, and that for free ion is denoted $\bar{N}^+$; the difference $N^+-\bar{N}^+$ is denoted ΔN^+.

The small wavelength region of interest in the present experiment is a good example of a region that resisted analysis until recently. This region contains Rydberg states with principal quantum numbers ranging from 4 [described by Hund's case (b)] to 9 [intermediate between Hund's cases (b) and (d)]. Although the wavelength resolution used in these experiments (typically 0.18 Å) permitted only partial resolution of the Rydberg structure in this region, it is important to understand all of the structure in the region in order to discuss the present results. For this reason, we include a small portion of the results from earlier work of Dehmer and Chupka.[6] Figure 1 shows the relative photoionization cross section of H_2 taken at a wavelength resolution of 0.016 Å and at 78 K. In that experiment, the room temperature equilibrium ortho–para mixture was quickly cooled to liquid nitrogen temperature, and there was no significant ortho–para conversion; only two rotational levels of H_2 had significant population—$J''=0$ (24.8%) and $J''=1$ (75.0%). In contrast, the data reported in the present study were taken at room temperature (300 K) and have a larger distribution of ground state rotational levels. Four rotational levels have significant population—$J''=0$ (13.1%), $J''=1$ (66.0%), $J''=2$ (11.6%), and $J''=3$ (8.8%).

Recent unpublished MQDT calculations[18] were used to assign the observed transitions from the $J''=0$ and 1 levels shown in Fig. 1; these transitions were only partially assigned when the spectrum was originally published by Dehmer and Chupka.[6] In addition, the calculations predict the wavelengths and approximate intensities of the transitions expected from the $J''=2$ and 3 levels. There are 24 transitions from these higher rotational levels, but only 3 have significant intensity in the room temperature spectrum. These transitions [and their intensities compared to

Downloaded 22 Aug 2006 to 129.6.168.231. Redistribution subject to AIP license or copyright, see http://jcp.aip.org/jcp/copyright.jsp

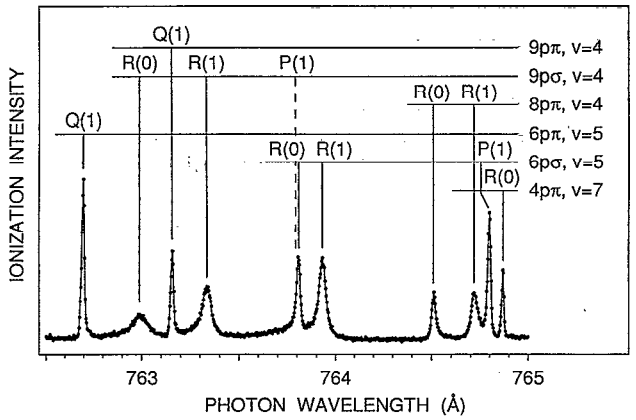

FIG. 1. Relative photoionization cross section of normal H_2 in the region of the $v^+=3$ ionization threshold, taken at 78 K and at a wavelength resolution of 0.016 Å. The data are from Ref. 6, and the assignments are from unpublished MQDT calculations of Pratt and Jungen (Ref. 18). All of the observed lines are accounted for by the calculations, and the predicted position of the unobserved $P(1)$ $9p\sigma$, $v=4$ transition is shown by a dashed line.

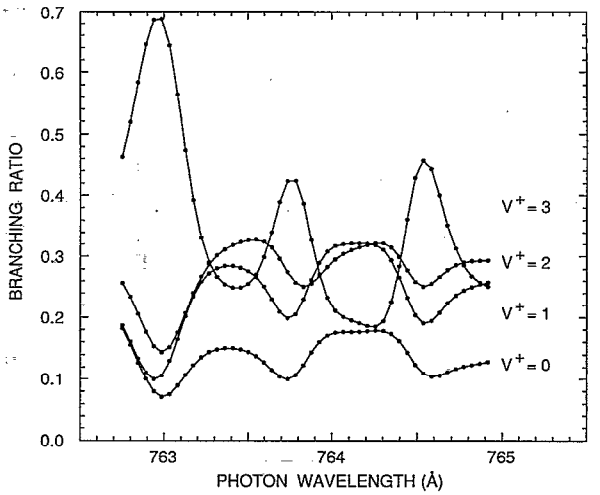

FIG. 2. Theoretical vibrational branching ratios (from Ref. 5) for photoionization of $H_2 X\,^1\Sigma_g^+$, $v''=0$, $J''=0$ in the region of the $v^+=3$ ionization threshold, convoluted with the 0.18 Å optical bandpass used in the present experiments. The solid dots indicate the mesh used for the convolution procedure.

that of the $R(1)$ $6p\sigma$, $v=5$ transition at 763.933 Å] are $Q(3)$ $5p\pi$, $v=6$ at 763.025 Å (25%); $R(2)$ $6p\sigma$, $v=5$ at 764.526 Å (13%); and $Q(3)$ $6p\pi$, $v=5$ at 764.830 Å (19%). All three of these transitions appear within a few hundredths of an Angstrom and are weaker than transitions observed from the $J''=0$ and 1 levels. Hence, since $J''=1$ is the most populated rotational level in both experiments and since transitions from $J''=2$ and 3 do not contribute substantial additional structure to that shown in Fig. 1, it is not surprising that the partial ionization cross sections reported in the present paper show three broad features corresponding approximately to a convolution of the three groups of peaks shown in the high-resolution spectrum of Fig. 1. Similarly, the total ionization cross section shows the same overall structure.

The region shown in Fig. 1 lies just above the $H_2^+ X\,^2\Sigma_g^+$, $v^+=3$ ionization threshold at 765.62 Å,[1] and the spectrum is characteristic of regions just above ionization thresholds in H_2. In particular, states with substantial $p\sigma$ character, low principal quantum number, and a vibrational quantum number that permits autoionization via $\Delta v=-1$ are known to have very fast autoionization rates and hence large halfwidths. The $np\sigma\,^1\Sigma_u^+$ states with the lowest values of n and v that lie just above an ionization threshold fulfill these requirements; in the region shown in Fig. 1, these states are the upper levels of the $R(0)$ and $R(1)$ $9p\sigma$, $v=4$ transitions. States with substantial $p\pi$ character [such as the upper levels of the $Q(1)$ transitions], high principal quantum numbers, or vibrational quantum numbers that require autoionization via $|\Delta v|>1$ have considerably slower autoionization rates and hence smaller halfwidths. All of these trends are seen qualitatively in the transitions shown in the total ionization cross section in Fig. 1. The present work now seeks to go beyond this level of understanding by examining the spectral variation of the branching ratios and the asymmetry parameters.

B. Branching ratios

Above the $v^+=3$ ionization limit, there are four open vibrational ionization continua, $v^+=0$ to 3. In the open continuum (i.e., in regions free from autoionizing states, shape resonances, and thresholds), the branching ratio for direct photoionization into a given vibrational continuum, v^+, is given approximately by the ratio of the Franck–Condon factor for the $X\,^1\Sigma_g^+$, $v''=0\rightarrow X\,^2\Sigma_g^+$, v^+ ionizing transition to the sum of the Franck–Condon factors for the $X\,^1\Sigma_g^+$, $v''=0\rightarrow X\,^2\Sigma_g^+$, $v^+=0$–3 ionizing transitions. These branching ratios are 0.16, 0.28, 0.30, and 0.26 for $v^+=0$–3, respectively. However, in the vicinity of autoionizing Rydberg states, marked deviations from the Franck–Condon approximation are to be expected, since ionization occurs via an indirect mechanism involving a transfer of vibrational excitation of the molecular core to the Rydberg electron during a close collision. Under these circumstances, the branching ratio is no longer governed by the vibrational overlap between the initial $X\,^1\Sigma_g^+$, $v''=0$ and final $X\,^2\Sigma_g^+$, v^+ states, but rather by the matrix elements coupling the autoionizing Rydberg state with the final $X\,^2\Sigma_g^+$, v^+ states. When the potential energy curves of the Rydberg and ionic states are similar, as is the case for H_2, it is well known that vibrational autoionization strongly favors the minimum change in vibrational quantum number of the molecular core.[4,5,7]

To illustrate the effect of vibrational autoionization on vibrational branching ratios for H_2 in this spectral range, we present in Fig. 2 the MQDT calculation of Raoult and Jungen[5] for para-H_2; the theoretical results have been convoluted with the 0.18 Å resolution used in the present measurement. These calculations consider only transitions from $J''=0$, i.e., they consider only $R(0)$ transitions. Specifically, the wavelength range of the calculations includes three of the four $R(0)$ transitions shown in Fig. 1—$R(0)$

Downloaded 22 Aug 2006 to 129.6.168.231. Redistribution subject to AIP license or copyright, see http://jcp.aip.org/jcp/copyright.jsp

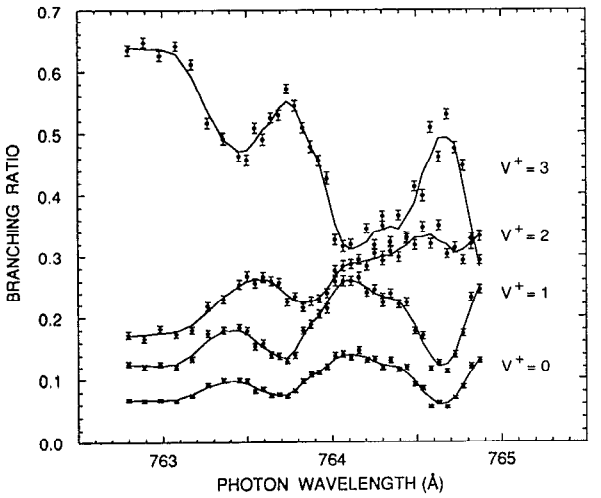

FIG. 3. Experimental vibrational branching ratios for photoionization of $H_2X\ ^1\Sigma_g^+$, $v''=0$, J'' in the region of the $v^+=3$ ionization threshold, taken at room temperature and at a wavelength resolution of 0.18 Å. The solid lines through the data points are smoothed curves intended to help visualize the overall shape of the experimental data.

$9p\sigma$, $v=4$ at 763.00 Å; $R(0)$ $6p\sigma$, $v=5$ at 763.78 Å; and $R(0)$ $8p\pi$, $v=4$ at 764.50 Å. Since the present measurements used room-temperature, normal H_2, the calculation of Raoult and Jungen[5] cannot be compared directly with the experimental results presented below. However, the calculations are included here to illustrate the main qualitative effects of vibrational autoionization. For nonresonant ionization, the branching ratios in Fig. 2 agree qualitatively with the Franck–Condon factors, as anticipated above. However, the agreement cannot be expected to be very good, since this small wavelength region is near an ionization threshold and contains three resonant transitions; therefore it cannot be considered an open continuum. The effects of vibrational autoionization are clearly seen at the wavelengths of the $R(0)$ transitions. Specifically, at each resonance, the vibrational channel corresponding to the minimum change in vibrational state of the molecular core exhibits a maximum, while the vibrational channels corresponding to larger changes in vibrational quantum number exhibit minima. Considerably more detail is present in the unconvoluted MQDT results originally published by Raoult and Jungen,[5] including examples of breakdown of the propensity rule; however, the qualitative behavior at the vibrational level is the most relevant to the data discussed below.

The branching ratios measured in this spectral range for normal H_2 at room temperature are presented in Fig. 3. In discussing these results, we emphasize transitions from $J''=1$, since $J''=1$ represents 66.0% of the sample; however, as noted above, $J''=0$, 2, and 3 are present in amounts ranging from 9% to 13%. Despite the differences in the initial rotational distribution for theory and experiment, the data in Fig. 3 show the same qualitative features as do the theoretical branching ratios. Evidence for three separate groups of unresolved autoionizing resonances is observed. In each case the $v^+=3$ branching ratio peaks and the others dip. The longest wavelength feature occurs at approximately 764.75 Å, the position of the $R(1)$ $8p\pi$, $v=4$ and $P(1)$ $6p\sigma$, $v=5$ transitions. The behavior seen here is qualitatively quite similar to that shown by the theoretical branching ratios near the $R(0)$ $8p\pi$, $v=4$ transition. The same behavior is observed at approximately 763.8 Å, presumably because of the combined effects of the $R(0)$ and $R(1)$ $6p\sigma$, $v=5$ transitions. At still shorter wavelengths, the experimental branching ratios show evidence for a third group of unresolved autoionizing resonances, presumably the $R(0)$ and $R(1)$ $9p\sigma$, $v=4$ and $Q(1)$ $9p\pi$, $v=4$ transitions. The branching ratio for $v^+=3$ remains high at the short wavelength end of the scan shown in Fig. 3 because of the effects of the $Q(1)$ $6p\pi$, $v=5$ transition.

In the data shown in Fig. 3, the branching ratios between the groups of resonances do not return to the Franck–Condon predictions for ionization in an open continuum due, at least in part, to the presence of $J''=0$ to 3 in the sample gas. Nevertheless, we conclude that the branching ratios presented here reflect, at the vibrational level, the qualitative behavior predicted by Raoult and Jungen.[5] Although the rotational structure is not resolved, the energy shifts and the differences between the experimental and theoretical branching ratios appear consistent with the known transitions in this region. Ultimately, of course, a quantitative comparison of this type will require further theoretical and experimental progress as discussed below.

C. Angular distributions

Photoelectron angular distributions depend not only on the dipole amplitudes of the partial waves of the outgoing electron but also on the interference among these partial waves, which in turn depends on their relative phases. Photoelectron angular distributions are thus complementary to and reflect the decay of dynamics of the autoionizing Rydberg state differently than do the vibrational branching ratios. Values of the asymmetry parameter β are bounded by geometry to lie between the limits of $\beta=-1$ and $\beta=2$.[19] Due to the interference nature of asymmetry parameter, spectral variations in β caused by autoionizing resonances need not be centered at the resonance position or have the same resonance width as the spectral variation observed in the photoabsorption and photoionization cross sections. Photoelectron angular distributions also show how the angular momentum carried by the incoming photon is apportioned between the ejected electron and the residual ion core.

The physical interpretation of molecular photoelectron angular distributions is particularly transparent for photoionization of para-H_2 in the $J''=0$ rotational level. Paraphrasing from Ref. 5, if we assume that the photoelectron escapes as a p wave (an excellent assumption in this spectral range), the angular distribution is completely determined, independent of dynamics, by the rotational level of the residual ion, i.e., $\beta(\bar{N}^+=0)=2$ and $\beta(\bar{N}^+=2)=1/5$.[5,20] Hence, if the angular momentum carried by the photon is transferred directly to the excited electron, which escapes with $l=1$ and leaves the ion core in its ground

Downloaded 22 Aug 2006 to 129.6.168.231. Redistribution subject to AIP license or copyright, see http://jcp.aip.org/jcp/copyright.jsp

state, the photoelectron angular distribution would have $\beta=2$. In fact, the value of β is very near this limit for nonresonant wavelengths. This can be viewed as the rotational analog of the vibrational Franck–Condon principle, which states, in essence, that in electronic transitions the slowly vibrating nuclei play the role of spectators. For direct (nonresonant) photoionization of $J''=0$, small departures from $\beta=2$ reflect the degree to which collisions between the outgoing electron and the anisotropic core lead to the exchange of angular momentum between the electron and the core, resulting in production of the "forbidden" $\overline{N}^+=2$ ionization channel. For resonant photoionization, on the other hand, the quasibound nature of the autoionizing resonance provides a greater opportunity for the excited electron to transfer angular momentum to the ion core through repeated collisions between the outgoing electron and the core. This produces rotationally excited molecular ions and reduces the asymmetry of the photoelectron angular distribution. Note that this process conserves angular momentum, unlike the common misconception that long lived autoionizing states somehow "forget" the angular information imparted during the photoabsorption process. Note also that the reduction in photoelectron asymmetry for autoionization of resonant transitions is not a general trend for all resonances; indeed, photoelectron asymmetries may be greater on resonance than off-resonance, depending on the specific dynamics of a particular case.

These ideas are illustrated in the theoretical results near the $v^+=3$ ionization limit shown in Fig. 4. Recall that the calculation in Ref. 5 included three $R(0)$ transitions at approximately 763.00, 763.78, and 764.50 Å. This is a relatively high density of resonances, so the region studied does not give a good example of direct, nonresonant photoionization. Nevertheless, for those channels that do not couple strongly with the vibrational autoionizing resonances, the asymmetry parameters approach the limit of 2, which indicates that ions are being formed in $\overline{N}^+=0$, i.e., without a change of the rotational state of the ion core during the photoionization process. However, in the vicinity of the three $R(0)$ resonances, prominent dips occur in the β parameter for $v^+=2$ and 3, indicating a reduced degree for anisotropy in the photoelectron angular distribution and, therefore, increased population of $\overline{N}^+=2$ residual ions. The unconvoluted theory curves of Raoult and Jungen[5] display values of β much closer to the value of 1/5 expected for pure $\overline{N}^+=2$ ionization.

Two other characteristics of β curves described above are observed in the theoretical curves. First, as described above, the extrema in the wavelength dependence of β for different v^+ need not have the same wavelengths as one another or as those of the branching ratios. This is most clearly seen for the $R(0)$ $8p\pi$, $v^+=4$ resonance at 764.50 Å. Second, the influence of the resonances on the wavelength dependence of β may extend well beyond the width observed in the total or partial cross sections for ionization channels that are coupled strongly to the resonances. For autoionization via minimum change in Δv [for the two $R(0)$ transitions having $v=4$, the minimum change in Δv is -1], the deviations from the nonresonant value of $\beta=2$ extend far beyond the resonance, so that this curve in Fig. 4 does not return to the nonresonant value between the resonances. These deviations are less for larger changes in Δv, and the deviations are quite small for the largest changes in Δv as exemplified by the β curves for $v^+=0$ and 1. This behavior is displayed much more clearly in the unconvoluted theoretical results of Raoult and Jungen (see Fig. 5 of Ref. 5).

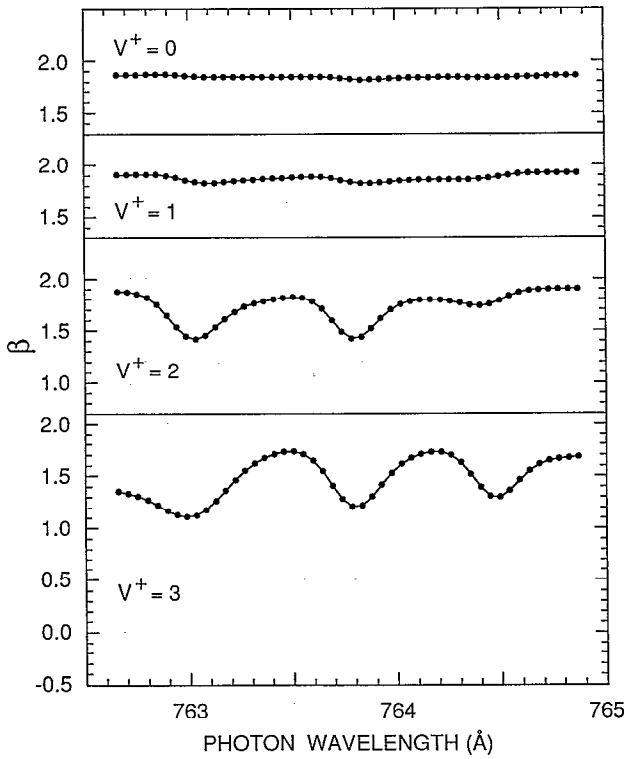

FIG. 4. Theoretical asymmetry parameters β (from Ref. 5) for photoionization of $H_2X\,^1\Sigma_g^+$, $v''=0$, $J''=0$ in the region of the $v^+=3$ ionization threshold, convoluted with the 0.18 Å optical bandpass used in the present experiments. The solid dots indicate the mesh used for the convolution procedure.

The present measurements of the spectral variation of the asymmetry parameter β for normal H_2 at room temperature are given in Fig. 5. As with the branching ratios, the experimental results qualitatively show the characteristics found in the theoretical calculations. For example, the β curves for $v^+=0$ and 1 lie close to the nonresonant value of $\beta=1.92$ at all wavelengths, demonstrating only weak coupling of these ionization channels to the autoionizing resonances. Also, the β curves for $v^+=2$ and 3 curves show a progressive loss of anisotropy near the resonances due to angular momentum transfer between the Rydberg electron and the ion core. However, beyond these qualitative similarities, there appear significant differences due to the additional rotational levels populated in the experiment. For example, in the β curve for $v^+=2$ curve, the minimum at 763.8 Å is remarkably similar in the theoretical and experimental curves, whereas the corresponding minima at 763.0 and 764.5 Å show significant differences

Downloaded 22 Aug 2006 to 129.6.168.231. Redistribution subject to AIP license or copyright, see http://jcp.aip.org/jcp/copyright.jsp

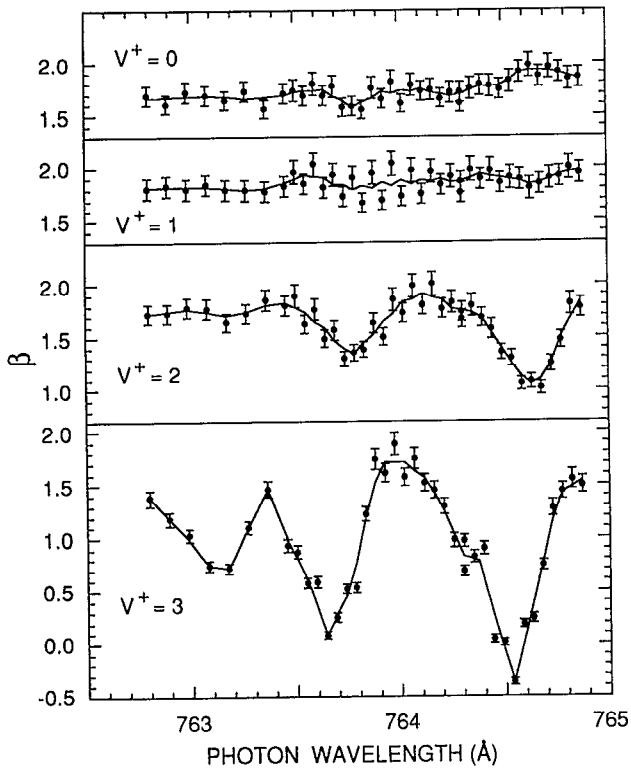

FIG. 5. Experimental asymmetry parameters β for photoionization of $H_2X\,^1\Sigma_g^+$, $v''=0$, J'' in the region of the $v^+=3$ ionization threshold, taken at room temperature and at a wavelength resolution of 0.18 Å. The solid lines through the data points are smoothed curves intended to help visualize the overall shape of the experimental data.

in amplitude and position. In the β curve for $v^+=3$, the differences between theory and experiment are even more pronounced. For example, the experimental β curve drops significantly below the value of 1/5, which is the minimum value allowed for photoionization of para-H_2 in the $J''=0$ rotational state. This is not surprising, since values of β for larger values of J'' can vary over the full range available to β. Indeed, a calculation near the $v^+=1$ ionization limit for $J''=1$ shows a similar variation.[21] However, we again note that the experimental β curve for $v^+=3$ was normalized to the theoretical curve at the endpoints of the wavelength scan, which limits the absolute accuracy of the former. Clearly, the experimental β curve for $v^+=3$ should be renormalized after an MQDT calculation of all of the rotational levels present in room-temperature, normal H_2.

IV. CONCLUSIONS

Vibrational branching ratios and photoelectron angular distributions are reported for photoionization of H_2 in the region of vibrationally autoionizing states just above the $v^+=3$ ionization limit. The main characteristics of vibrational autoionization predicted by Raoult and Jungen[5] are observed, namely, the propensity for decay by the minimum change in the vibrational state of the ion core and the strong reduction of the photoelectron asymmetry in the vicinity of a resonance. A quantitative comparison is not possible at this time, since the existing theoretical calculation was limited to ionization from $J''=0$, while the present experiment included ionization from $J''=0$–3. We hope that this study will stimulate two additional efforts—first, the extension of MQDT calculations to room temperature H_2 so that a direct comparison with the present results can be made and second, the determination of branching ratios and angular distributions at higher wavelength resolution by using third-generation synchrotron radiation sources to match the level of detail provided by theory.

ACKNOWLEDGMENTS

We would like to thank Stephen T. Pratt and Christian Jungen for providing us with the results of their MQDT calculations prior to publication. This work was supported in part by the U.S. Department of Energy, Office of Energy Research, Office of Health and Environmental Research, under Contract No. W-31-109-ENG-38.

[1] G. Herzberg, *Molecular Spectra and Molecular Structure, Volume I, Spectra of Diatomic Molecules* (Van Nostrand, New York, 1950).
[2] J. Franck, Trans. Faraday Soc. **21**, 536 (1925); E. U. Condon, Phys. Rev. **32**, 858 (1928).
[3] M. Born and R. Oppenheimer, Ann. Phys. **84**, 457 (1927).
[4] G. Herzberg and Ch. Jungen, J. Mol. Spectrosc. **41**, 425 (1972).
[5] M. Raoult and Ch. Jungen, J. Chem. Phys. **74**, 3388 (1981).
[6] P. M. Dehmer and W. A. Chupka, J. Chem. Phys. **65**, 2243 (1976).
[7] R. S. Berry and S. E. Nielsen, Phys. Rev. A **1**, 383, 395 (1970).
[8] J. Berkowitz and W. A. Chupka, J. Chem. Phys. **51**, 2341 (1969).
[9] P. M. Dehmer and W. A. Chupka, J. Chem. Phys. **66**, 1972 (1977).
[10] M. A. O'Halloran, P. M. Dehmer, F. S. Tomkins, S. T. Pratt, and J. L. Dehmer, J. Chem. Phys. **89**, 75 (1988).
[11] A. C. Parr, S. H. Southworth, J. L. Dehmer, and D. M. P. Holland, Nucl. Instrum. Meth. **222**, 221 (1984).
[12] D. M. P. Holland, J. B. West, A. A. MacDowell, I. H. Munro, and A. G. Beckett, Nucl. Instrum. Meth. B **44**, 233 (1989).
[13] J. B. West and H. A. Padmore, in *Handbook on Synchrotron Radiation*, edited by G. V. Marr (North Holland, Amsterdam, 1987), p. 21.
[14] V. G. Horton, E. T. Arakawa, R. N. Hamm, and M. W. Williams, Appl. Opt. **8**, 667 (1969).
[15] J. A. R. Samson and A. F. Starace, J. Phys. B **8**, 1806 (1975).
[16] J. J. Hopfield, Nature (London) **125**, 927 (1930).
[17] U. Fano, Phys. Rev. A **2**, 353 (1970).
[18] S. T. Pratt and Ch. Jungen (private communication, 1992).
[19] C. N. Yang, Phys. Rev. **74**, 764 (1948).
[20] Dan Dill, Phys. Rev. A **6**, 160 (1972).
[21] M. Raoult, Ch. Jungen, and D. Dill, J. Chim. Phys. (Paris) **77**, 599 (1980).

Downloaded 22 Aug 2006 to 129.6.168.231. Redistribution subject to AIP license or copyright, see http://jcp.aip.org/jcp/copyright.jsp